Indian Journal of Pure & Applied Physics
Vol. 60, April 2022, pp. 313-319

Analyzing the Suitability of Chromium Doped Iron Oxide Nanoparticles for Creatinine Bio Sensor Applications

Priyadharshini Muthukumaravel[a*], Rajesh Pattulingam[a], Manikandan Jeganathan[b], Hariharan Venkatesan[c] & Ezhil Inban Manimaran[d]

[a]Department of Chemistry, Government Arts College, Coimbatore-641 018, Tamilnadu, India
[b]Department of Chemistry, Government Arts College, Coimbatore-641 018, Tamilnadu, India
[c]Department of Physics, Mahendra Arts and Science College, Namakkal-637 501, Tamilnadu, India
[d]Department of Physics, Government Arts College, Coimbatore-641 018, Tamilnadu, India

Received 16 January 2022; accepted 23 March 2022

The present work focused on the synthesis and characterization of Cr (~2, 3 & 5 wt.%) doped Fe_2O_3 nanoparticles with desired electrochemical property for creatinine bio sensor applications via the extraction of *Nyctanthes arbor tristis* seed by facile chemical precipitation method. The synthesized samples have dimensions of the order of 0.5 to 0.8 μm and crystallite size of the prepared samples calculated by Powder XRD analysis using Scherer's formula. The optical characterization of the prepared nanomaterials showed that the band gap energy of the annealed chromium doped samples were found to be 5.74 eV by varying in intensity by Tauc plot that established well optical nature of the synthesized compound which is also have a good concord with the Powder XRD analysis with its crystalline nature. The FT-IR spectra clearly indicating the complete formation of Fe_2O_3 by observing corresponding functional groups such as Fe=O and O=O vibrations in their respective wavenumbers. The sensing performance of the prepared samples for creatinine was carried out using electrochemical workstation. Interestingly, the electrochemical analysis exposed the good sensing behaviour of the Cr-doped Fe_2O_3 nanoparticles which displayed corresponding redox peaks attributed to the reversible Faradaic redox reaction at the electrode surface caused by the pseudo-capacitance nature for α – Fe_2O_3 nanoparticles as an active material, slightly than the double layer capacitance. Consequently the current outcomes revealed a good sensing behaviour on creatinine for Cr-doped Fe_2O_3 nanoparticles synthesized by an effortless cost effective green synthesis method.

Keywords: Iron oxide, Cr-doped, *Nyctanthes arbor tristis*, Nanomaterials, Creatinine

1 Introduction

Synthesizing materials by using number of components or unit operations to fabricate elements with distinct properties is known as Nanotechnology which can be utilized in different applications. Nanoparticle is defined as small particles having dimensions between 1-100 nm. They own special optical, thermal and electrochemical properties disparate from that of the bulk materials due to their compact particle size[1]. These nanoparticles play an important role in the field of biomedical and industrial evolution due to their very high surface to volume ratio. A metal oxide shows the potential to shape wider range of oxide compounds so they are employed in numerous aspects of physics, chemistry and materials science. They can expose metallic, semiconductor and insulator features and fit to an enormous structural geometry. Owing to their high density and controlled size, delicate physical and chemical properties are shown by them[2].

*Corresponding author: (E-mail: dharshinimuthu93@gmail.com)

Iron oxide nanoparticles are considered as the most significant metal oxide nanoparticles among numerous nanoparticles on the basis of their prominent aspects like bio compatibility and magnetic property[3]. Beside various phases, hematite (α-Fe_2O_3), maghemite (γ - Fe_2O_3), magnetite (Fe_2O_3) are the frequently used and maximum considered phases of iron oxides. The hematite (α - Fe_2O_3) is considerably used in different inorganic applications like catalysis, sensing etc., due to their extreme stability in natural environmental conditions[4]. The familiar predominant polymorph of iron oxide is hematite and they are generally found in rocks and soils which survive in nature in the form of minerals. At room temperature, it shows weak ferromagnetic or anti ferromagnetic activity. It displays a rhombohedral structure similar to that of corundum which composed of O^{2-} ion reticle as a close-packed hexagonal crystallographic system and two thirds of the octahedral interstices was inhabited by Fe^{3+} ions in alternate layers. Transformation of various iron oxide

forms results in the formation of hematite as the final product so that effortlessly we can synthesis α-Fe_2O_3 than the other oxide forms[5].

The morphology of α-Fe_2O_3 nanoparticles plays a vital role in their physicochemical properties and their pursuance in distinct applications. To modify their morphology and enhance their properties hematite nanoparticles were doped with various metal ions such as Mn, Cu, Co, Al, Cr etc., and hinge on the valence state along with ionic radius by a very simple and cost-effective method. Concerning, trivalent cations are significant[6]. An appropriate cation for integration into the crystal structure of hematite is a trivalent chromium ion (Cr^{3+}) which substituted the Fe^{3+} ion as a consequence of identical ionic charge and corresponding ionic radius (0.615 Å and 0.645 Å for Cr^{3+} and Fe^{3+}). Chromium (III) oxide eskolaite (Cr_2O_3) is iso structural with hematite (Corundum-type crystal structure). It is a hopeful aspirant for effective doping substances in sensor operations[7].

Synthesis of nanoparticles is carried out by various physical and chemical procedures which employ toxic solvents that are insecure and cause hazardous by products. Furthermore, the synthesis of these nanoparticles requires high energy utilization that results in toxicity in the environment[8]. Therefore to overcome the ejection of hazardous by products found in chemical synthesis, the green synthesis of nanoparticles acquired ample support as it make use of non-toxic phytochemicals. In green synthesis method, the utilization of plant extract from various parts of the plant acts as the reducing and stabilizing agents that reduces metal salts into metal nanoparticles in a short time as well as the production of nanoparticles are carried out at large scale by a very simple, easy process in an effective manner[9]. The non-toxic and amiable seed extract of *Nyctanthes Arbor Tristis* plant was used for the synthesis of α-Fe_2O_3 nanoparticles[10]. It is a mythological plant which refers to *Oleaceae* species and they own high medicinal values.

Creatine is an amino acid derivative which is synthesized from L-arginine, glycine and S-adenosylmethionine in the kidneys, liver and pancreas. The creatine level in blood serum and urine is clinically used as a parameter of muscle damage. Hence, an accurate and rapid determination of creatine concentration is significant. Majority of the methods for creatine and creatinine determination are generally laborious, expensive, time-consuming and complex to perform. Alternatively, biosensors allowing direct measurements of creatine in sample, promise economy of time and saving of costs in pharmaceutical and clinical analysis. To obtain a high-performance creatinine biosensor utilization of nanoparticles is awfully attractive. In recent times, a range of nanomaterials have found numerous applications in biosensor applications[11].

The aim of this study are to (i) Synthesize chromium doped α - Fe_2O_3 nanoparticles using seed extract of *Nyctanthes Arbor Tristis* (ii) Characterize synthesized 'Cr' doped α - Fe_2O_3 NPs (iii) Determine the suitability of 'Cr' doped α-Fe_2O_3 NPs for Creatinine biosensors.

2 Materials and methods

The precursors such as $FeCl_3$, aqueous NH_3 and $Cr_2(SO_4)_3$ was bought from Merck with analytical grade as well as utilized as such unless any further purification.

2.1 Extraction of plant material

The seeds of *Nyctanthes arbor tristis* plant was collected, separated from shell, dried and made into powder form. 10 grams of powdered seed was weighed and added to 100 ml of deionized water taken in a 250 ml glass beaker. The mixture was stirred continuously for 2 hours using a magnetic stirrer kept at room temperature. The solution was allowed to settle for some time and then the extraction was filtered using a whatman filter paper. The freshly prepared extract was used for the preparation of Cr - doped Fe_2O_3 nanoparticles.

2.2 Preparation of iron oxide nanoparticles

4.055 g of $FeCl_3$ (0.5 M) was added to 50 ml of the extract and stirred for 2 hours at room temperature using a magnetic stirrer. After 2 hours, 10 ml of aqueous ammonia solution was added drop wise in order to maintain the pH of the solution for around 10-12 and again stirred for an another 1 hour. A reddish brown precipitate was obtained. The iron oxide solution was collected, filtered and washed several times with double distilled water to detach chloride ions present in the precursor. The filtered precipitate was dried using a hot air oven for 60 ºC in air. The final product was transferred to a muffle furnace and kept at 600 ºC in air for 6 hours. The resultant reddish brown powder was undergone for further characterization in order to know the suitability of the material for sensor applications.

2.3 Preparation of 'Cr' doped iron oxide nanoparticles

The procedure adopted for the synthesis of iron oxide nanoparticles remains same for the preparation

of 'Cr' (~ 2, 3 & 5 wt.%) doped solution. $Cr_2(SO_4)_3$ was weighed and added to 50 ml of deionised water. This solution will be kept under stirring process for 2 hours and transferred into a burette to carry out further process. The solution was added drop wise to the iron oxide solution and again stirred for 1 hour to obtain 'Cr' (~ 2, 3 & 5 wt.%) doped iron oxide nanoparticles. The supernatant solution was removed and washed several times in order to remove the impurities. The precipitate was dried using a hot air oven for 60 ºC in air and kept in a muffle furnace at 600 ºC in air for 6 hours in order to remove the impurities and also to improve the crystallinity of the resultant product.

3 CharacterizationTechniques

The synthesized 'Cr' doped iron oxide nanoparticles are characterized by the following techniques. The phase formation and purity of the samples are analyzed by Bruker D8 Advanced X-ray diffractometer in Bragg Brentano geometry through Cu K-alpha radiation (λ = 1.5406 Å). To confirm the nature of the functional groups of the prepared materials, Bruker alpha FT-IR Spectrometer was used. Utilizing Cary 8454 UV-Vis Spectrophotometer the optical behavior of the iron oxide sample were observed. The surface morphology of the samples was studied *via* FE-SEM (HITACHI S-3400). The size of the synthesized samples was confirmed by Transmission Electron Microscopy (TEM). To find the effective surface area of the prepared nanomaterials, Brunauer-Emmett-Teller (BET) surface area analysis was utilized. Charge-discharge method and the electrochemical performance of cyclic voltammeter (CV) were carried out with CHI 604C potentiostat in a three electrode assemblage.

4 Results and discussion

4.1 Powder X-Ray Diffraction analysis

The structure state and the crystalline nature of the Cr-Fe_2O_3 nanoparticles were investigated by XRD analysis. Fig. 1 shows the XRD patterns of various concentrations of Cr-Fe_2O_3 nanoparticles. XRD patterns of the deposited Cr-Fe_2O_3 nanoparticles reveal the presence of polycrystalline Cr-Fe_2O_3 corresponding to cubic structure and without any secondary phases were observed, neither Fe_2O_3 nor Fe. Apart from the peaks corresponding Cr-Fe_2O_3 peaks are at 2θ values of 29.35°, 36.60°, 42.44° and 61.57° corresponding to (1 1 0), (1 1 1), (2 0 0) and (2 2 0) diffraction planes, respectively. This XRD results are in good agreement with the JCPDS card No. 05-0667 of Fe_2O_3 compound. The average crystallite size was calculated using the Debye Scherer equation and was found to be 16 ± 5 nm.

4.2 UV-Vis Spectroscopic Studies

The optical properties of the 2, 3 and 5% chromium doped iron oxide nanoparticles were analysed using UV-visible spectroscopic analysis. The outcome from that illustrates, the optical retention obtained around 212 nm and 214 nm for 2, 3 and 5% chromium doped iron oxide nanoparticles may be authorized to move towards blue locale as shown in Fig. 2.

It is to be seen that the relating retention absorption region 212 and 214 nm as 2%, 3% and 5% chromium doped iron oxide nanoparticles which certified the shift towards lower wavelength (blue shift) that is in simultaneousness with the powder XRD examination due to its formless and glasslike nature of the prepared materials. The determined energy band gap esteems for the Cr-doped iron oxide nanoparticles are considered to be 4.49, 4.91 and 5.74 eV separately using Tauc plot. It explains the validation for the blue

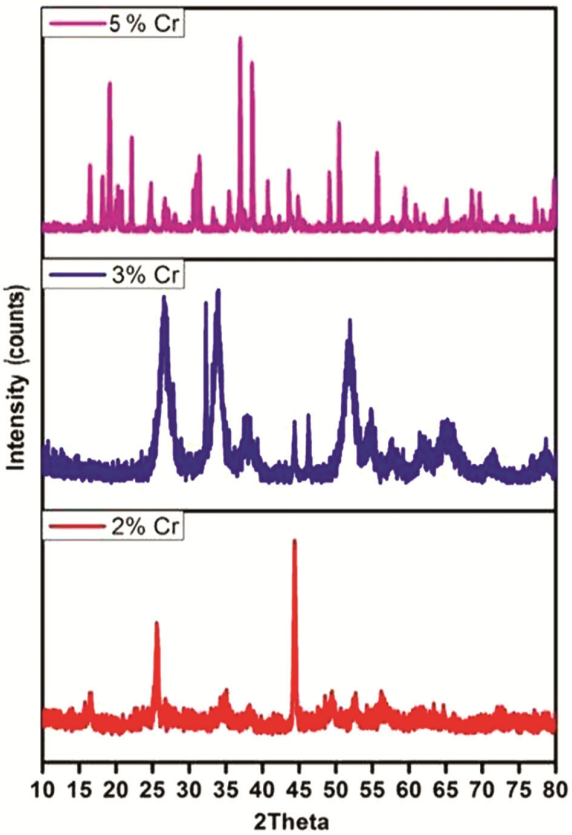

Fig. 1 — XRD pattern of 2%, 3% and 5% chromium doped iron oxide nanoparticles.

shift of the absorption curve in association with the lessening of the band gap energy.

4.3 FT-IR Analysis

Chromium ferrite nanoparticles functional groups were recognized by FT-IR spectroscopy. Fig. 3 shows the FT-IR range of chromium ferrite nanoparticles. The stretching and bending vibration of the two groups of metal oxide were seen in the scope of 559 cm^{-1} for 2, 3 and 5% chromium doped iron oxide nanoparticles. The presence of groups at 559 cm^{-1} in FT-IR range affirmed the arrangement of ferrite. The bending vibration was exceptionally expansive. The explanation could be ascribed to the appropriation of Fe^{3+} particles at tetrahedral locales. The stretching vibrations in the locales among 3437 cm^{-1} has a spot with -NH stretching and alkyl stretching vibrations independently that asserts the hint of extraction of the plants during the course of union. The pinnacles of assimilation around 1628, 1038 cm^{-1} are a result of the twisted and symmetric twisting vibration of C=O.

4.4 FE-SEM Analysis

A SEM micrographs with various amplifications of 2%, 3% and 5% chromium doped iron oxide nanoparticles displayed in Fig. 4 individually. From the SEM pictures, clearly the shape and size of nanostructures of the acquired powder can be identified with the synthesis interaction. The all micrographs show barely that the instances are existing as grains with little particles consistently on the surfaces. It is significant that while doping fixation changes from 2% to 5%, a perceptible expansion in grain size is noticed. The normal grain size for the specimen of 2%, 3% and 5% Cr-doped iron oxide nanoparticles are 0.5 to 0.8 µm. It is notable that a Cr-Fe_2O_3 nanoparticles with bigger grains and less grain limits are reasonable for biosensor applications on account of the conceivable decrease of recombination probability at the grain limits. Thus, to acquire an appropriate Cr-Fe_2O_3 nanoparticles, the voltammetry approach confirmation is a key for controlling the morphologies of the Cr-doped Fe_2O_3 nanoparticles.

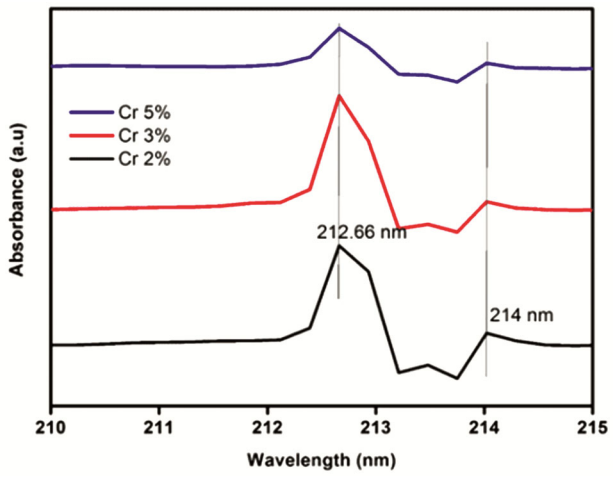

Fig. 2 — UV-Visible absorption spectrum of 2%, 3% and 5% chromium doped iron oxide nanoparticles.

4.5 HRTEM analysis

The TEM analysis was utilized to inspect different morphological spectrums, as displayed in Fig. 5 shows a low magnification TEM image of Cr-doped α-Fe_2O_3 nanoparticles from which the particle size is estimated to be 0.5 µm that possess polycrystalline structure. They exhibits a smooth surface and a relatively uniform diameter along the axial direction, using the high-resolution transmission electron microscopy (HRTEM) technique and it indicates the polycrystalline nature of α-Fe_2O_3 and is highly consistent with both the SEM and XRD results.

4.6 EDX analysis

The chemical composition of Cr (5%) doped Fe_2O_3 nanoparticles was further investigated by energy

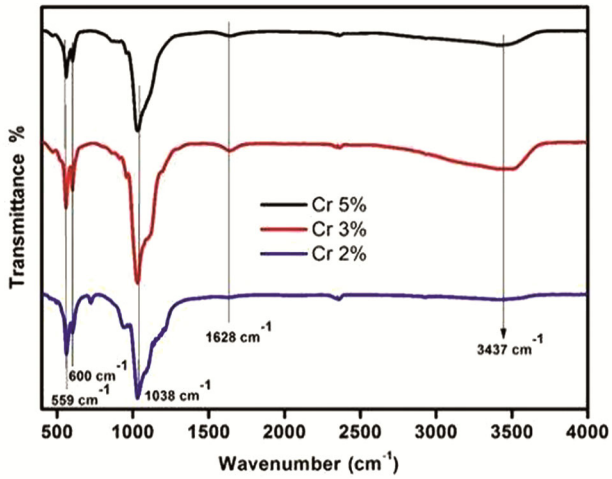

Fig. 3 — FT-IR spectra for 2%, 3% and 5% chromium doped iron oxide nanoparticles.

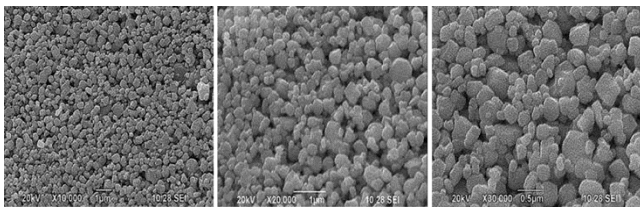

Fig. 4 — Microscopic images of 2%, 3% and 5% chromium doped iron oxide nanoparticles.

dispersive X-ray spectrum (Fig. 6). The EDX results corresponded to the XRD results demonstrate that sample is hexagonal wurtzite Fe_2O_3.The Table 1 shows chemical composition of Cr - doped Fe_2O_3.

4.7 BET Surface area analysis

To ascertain specific surface area of α-Fe_2O_3 and 'Cr' (~ 2, 3 & 5 wt.%) doped α-Fe_2O_3 nanoparticles, Brunauer–Emmett–Teller (BET) theory was adopted. The specific surface area of α-Fe_2O_3 is 34 m^2/g, which is greater than that of the commercially available iron oxide nanomaterials. The evaluated specific surface area for 'Cr' (~ 2, 3 & 5 wt.%) doped α-Fe_2O_3 samples by using BET analysis were found to be 12, 18.5 and 23.5 m^2/g (Fig. 7) which are lower than that of the iron oxide samples. The reduced specific surface area of chromium doped samples than the iron oxide samples may be owing to the difference in particle size distribution and particle shape between them as a consequence of doping which is in agreement with the above results. The iron oxides having higher concentration of the dopant (5 wt.%) own large specific surface area than the others because of the smaller particle size. In spite of bearing lower specific surface area than the undoped samples they demonstrate an enhanced electrochemical performance and high sensitivity as compared to the α-Fe_2O_3 samples without dopant[16].

Table 1 — Chemical composition of Cr-doped Fe_2O_3 nanoparticles

S. No	Elements	Mass%	Atomic%
1	O	36.83	66.61
2	Cr	23.35	11.65
3	Fe	39.82	21.74
	Total	100	100

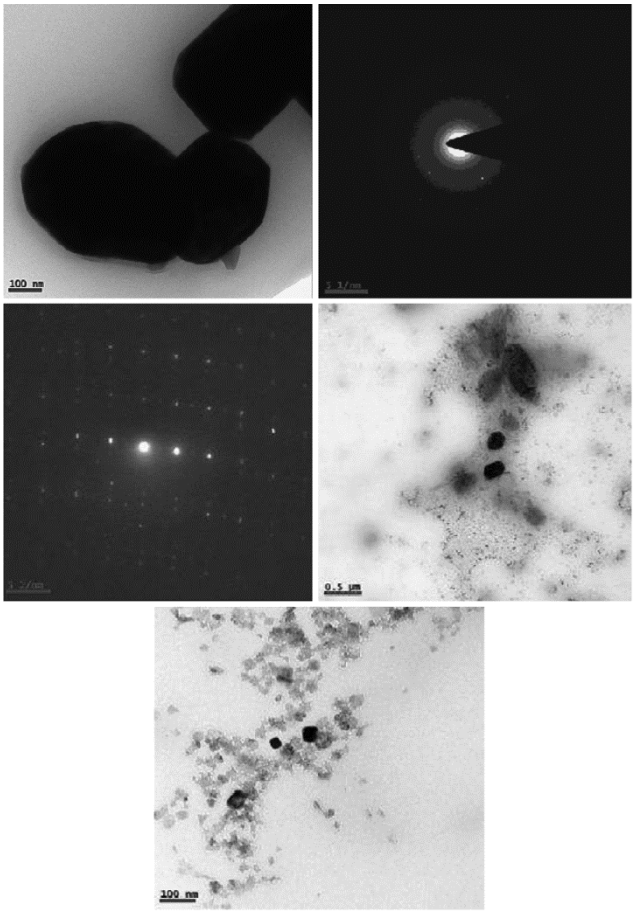

Fig. 5 — TEM images of 5% chromium doped iron oxide nanoparticles.

4.7 Electrochemical analysis

To investigate the sensitivity of Cr-doped α-Fe_2O_3 samples cyclic voltammetry was used. The electrochemical cell consists of three-electrodes in which the glassy carbon electrode as working electrode, platinum wire as reference electrode and

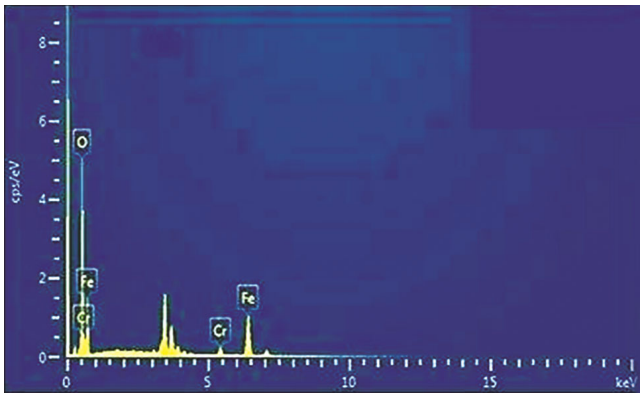

Fig. 6 — EDX analysis of Cr (5%) doped Fe_2O_3 nanoparticles.

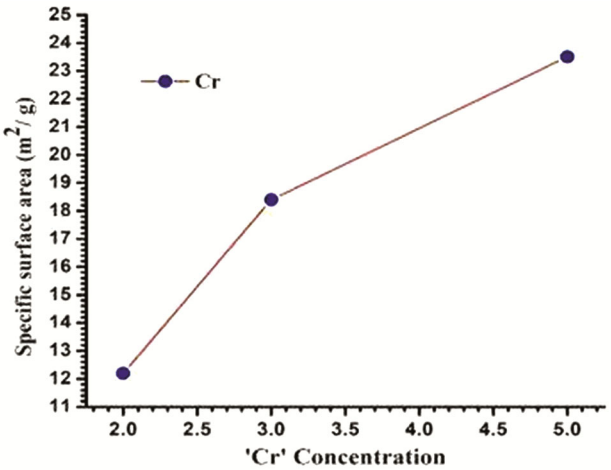

Fig. 7 — BET analysis of 5% 'Cr' doped iron oxide nanoparticles.

platinum foil as counter electrode. The Cr-doped Fe_2O_3 nanopowder was made into a paste using deionized water. The glassy carbon electrode was polished well and coated with the above paste with the help of the micro pipette. Cyclic voltammogram of the Cr-doped α-Fe_2O_3 modified electrode was recorded in presence of 0.5 mM creatinine solution. The potential was applied in the range of 0 to 1 volts utilizing three electrodes system in 1 M aqueous solution of $FeSO_4$ based electrolyte solution. The corresponding CV curves of the distinct electrodes were recorded with the sweep rates 10, 20, 40, 60 mVs^{-1} at room temperature. The corresponding attained peaks are may be due to the better correlation to the specific concentration of the specific electrolyte. Moreover, the oxidation and reduced peaks are due to specific concentration of creatinine is converted to its respective methylated form (Fig. 8) by an increasing its intensity peak. The linear increase in current signals confirmed detection of creatinine via the electrolyte.

The immobilized iron oxide gives rise to reduction peak at 0.2 V for the change in oxidation state of iron. The requirement of higher energy for conversion of Fe (III) to lower oxidation states is reflected by the increased shift of the reduction potential in the negative direction (Fig. 9). The cyclic voltammogram of Cr-doped iron oxide modified electrode indicated a reduction peak during the reversal potential sweep and associated oxidation peaks. The obtained redox potential displays good sensitivity and increased peak current in the case of 'Cr' doped α-Fe_2O_3 against 0.5 mM creatinine analyte. From the above results, we have concluded that 'Cr' doped α-Fe_2O_3 sample exhibit enhanced electrochemical performance and good sensitivity due to their higher surface area as compared to undoped α-Fe_2O_3 nanoparticles which is in agreement with the BET surface area analysis. The schematic representation of the process involved in creatinine biosensor was given below.

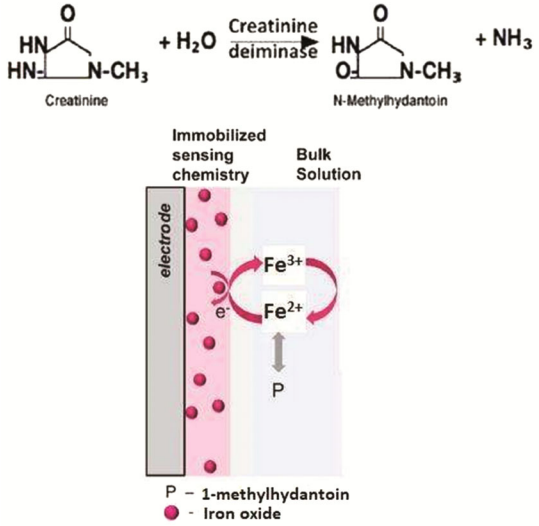

Fig. 8 — Electrochemical detection of 1-methylhydantoin.

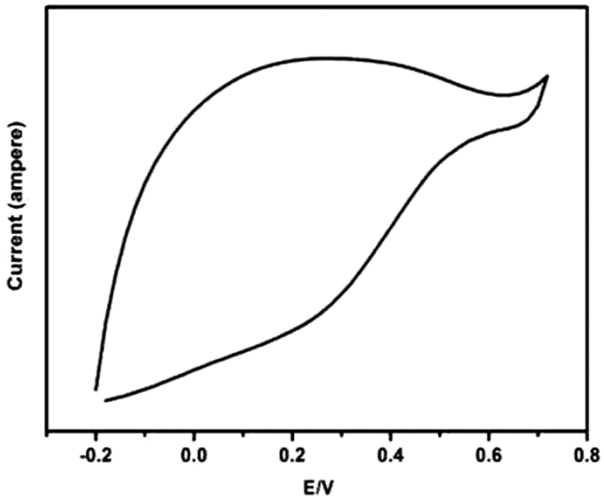

Fig. 9 — Electrochemical performance of 'Cr' doped Fe_2O_3 nanoparticles.

5 Conclusions

For the first time, eco-friendly Cr (~2, 3 & 5 wt.%) doped α-Fe_2O_3 samples were successfully synthesized with desired size and with comparatively large efficiency via *Nyctanthes arbor tristis* seed extract by facile chemical precipitation method. The synthesized samples have dimensions of the order of 0.5 to 0.8 μm which is in agreement with the FE-SEM, TEM and Powder XRD analysis. The determined band gap energy was found to be 5.74 eV by varying in intensity by Tauc plot that established well optical nature of the synthesized compound which is also have a good concord with the Powder XRD analysis. The FT-IR spectra clearly indicating the complete formation of Fe_2O_3 by observing corresponding functional groups such as Fe=O and O=O vibrations in their respective wave numbers. Interestingly, the electrochemical analysis exposed the good sensing behaviour of the Cr-doped Fe_2O_3 nanoparticles which displayed corresponding redox peaks attributed to the reversible Faradic redox reaction at the electrode surface caused by the pseudo-capacitance nature for α–Fe_2O_3 nanoparticles as an active material, slightly than the double layer capacitance. Consequently the current work demonstrated a good sensing behaviour

on Creatinine for Cr–doped Fe_2O_3 nanoparticles synthesized by an effortless cost effective green synthesis method.

References

1 Fahmy H M, Mohamed F M, Marzouq M H, Mustafa A B E D, Alsoudi A M, Ali O A & Mahmoud F A, *Bio Nano Sci*, 8 (2018) 491.

2 Vinayagam R, Selvaraj R, Arivalagan P & Varadavenkatesan T, *J Photochem Photobio B: Bio*, 203 (2020) 111760.

3 Anchan S, Pai S, Sridevi H, Varadavenkatesan T, Vinayagam R & Selvaraj R, *Biocat Agri Biotech*, 20 (2019) 101251.

4 Karade V C, Parit S B, Dawkar V V, Devan R S, Choudhary R J, Kedge V V & Chougale A D, *HeliYon*, 5 (2019) e02044.

5 Campos E A, Pinto D V B S, Oliveira J I S D, Mattos E D C & Dutra R D C L, *J Aerospace Tech Managmt,* 7 (2015) 267.

6 Riaz S, Bashir M & Naseem S, *IEEE Trans Mag*, 50 (2013) 1.

7 Popov N, Krehula S, Ristić M, Kuzmann E, Homonnay Z, Bošković M & Musić S, *J Phys Chem Sol,* 148 (2021) 109699.

8 Rahman S S U, Qureshi M T, Sultana K, Rehman W, Khan M Y, Asif M H & Sultana N, *Res Phys*, 7 (2017) 4451.

9 Singh J, Dutta T, Kim K H, Rawat M, Samddar P & Kumar P, *J Nanobiotech,* 16 (2018) 1.

10 Bhalakiya H & Modi N R, *Traditional Medicinal Uses, Phytochemical Profile and Pharmacological Activities of Nyctanthes Arbortris*, (2019).

11 Kaçar C, Erden P E, Pekyardimci Ş & Kiliç E, *Artif Cells Nanomed Biotech,* 41 (2013) 2.

12 Bouhjar F, Mollar M, Chourou M L, Marí B & Bessais B, *Electroch Act,* 260 (2018) 838.

13 Lassoued A, Lassoued M S, Dkhil B, Ammar S & Gadri A, *Phys E: Low-dimen Sys Nanostruc,* 101 (2018) 212.

14 Hwang S W, Umar A, Dar G N, Kim S H & Badran R I, *Sens Lett*, 12 (2014) 97.

15 Wang R, Liu H, Wang X, Li X, Gu X & Zheng Z, *Cat Sci Tech*, 10 (2020) 6483.

16 Oćwieja M Adamczyk Z & Kubiak K, *J Colloid Interf Sci,* 376 (2012) 1.